Hindawi Publishing Corporation
Journal of Nanomaterials
Volume 2012, Article ID 525616, 9 pages
doi:10.1155/2012/525616

Research Article

Parameter Optimisation of Carbon Nanotubes Synthesis via Hexane Decomposition over Minerals Generated from *Anadara granosa* Shells as the Catalyst Support

M. Z. Hussein,[1,2] S. A. Zakarya,[1] S. H. Sarijo,[3] and Z. Zainal[1,2]

[1] *Department of Chemistry, Faculty of Science, Universiti Putra Malaysia, Selangor, 43400 Serdang, Malaysia*
[2] *Advanced Materials and Nanotechnology Laboratory (AMNL), Institute of Advanced Technology (ITMA), Universiti Putra Malaysia, Selangor, 43400 Serdang, Malaysia*
[3] *Faculty of Applied Science, Universiti Teknologi MARA UiTM, Selangor, 40450 Shah Alam, Malaysia*

Correspondence should be addressed to M. Z. Hussein, mzobir@science.upm.edu.my

Received 8 April 2012; Accepted 10 July 2012

Academic Editor: Suprakas Sinha Ray

The synthesis of carbon nanotubes (CNTs) by the chemical vapour deposition (CVD) method using natural calcite from *Anadara granosa* shells as the metal catalyst support was studied. Hexane and iron (Fe) were used as the carbon precursor and the active component of the catalyst, respectively. Response surface methodology (RSM) based on central composite design (CCD) was used to optimise the effect of total iron loading, the duration of reaction, and reaction temperature. The optimal conditions were total iron loading of 7.5%, a reaction time of 45 min, and a temperature of 850°C with a resulting carbon yield of 131.62%. Raman spectra, field-emission-scanning electron microscopy (FESEM) and transmission electron microscopy (TEM) analyses showed that the CNTs were of the multiwalled type (MWNTs).

1. Introduction

The interest of materials science research on carbon nanotubes (CNTs) has grown tremendously since the first publication by Iijima in 1991 which evidenced the possibility of growing CNTs without the need of a catalyst [1]. Due to their myriad applications such as serving as anode materials in batteries [2], devices for hydrogen storage [3], electrodes in field-emission diodes [4], sensors for air-pollutant gases [5], and electrodes in capacitors [6], the parameters for controlling CNTs growth and cost reduction in CNTs production have been of interest.

Various synthesis methods have been developed such as electric arc discharge [7], pyrolysis [8], laser ablation [9], solvothermal [10], hydrothermal [11] and chemical vapour deposition (CVD) [12], and so forth. Among these methods, the CVD method has emerged as a powerful approach in allowing large-scale production of CNTs [13]. CVD is also the most promising method for a large-scale production of graphite fibres and multiwalled carbon nanotubes (MWCNTs) at a much lower temperature and hence reduce the cost of CNTs production [14].

In the CVD process the selection of a metallic catalyst may affect the growth and morphology of the nanotubes. Widely used catalyst materials in carbon nanotubes synthesis are cobalt, iron, titanium, nickel, a number of zeolites, and combinations of these metals and/or oxides. Generally, the catalyst metal particles or their compounds are uniformly dispersed on supports. This support plays an important role in influencing the activity of the catalyst [15].

Recently, natural minerals such as lava rock [16], marine manganese nodules [17] and fly ash [18] have been used as catalyst supports for the synthesis of nanocarbons. Not only the CNTs growth on natural materials is a low-cost and environmentally beneficial approach, but the supports from minerals, specifically calcite as used in this study, are also easily removed by acid treatment and tend to produce pure final product [19].

The process optimisation of CNTs synthesized via hexane decomposition over natural calcite from *Anadara granosa* shells using response surface methodology (RSM) is reported in the current study. The objectives of this work were to optimise the reaction conditions for CNTs production from

hexane decomposition over natural calcite from marine shells and to promote the commercial application of this biological waste.

2. Materials and Methods

2.1. Catalyst Support Preparation. Anadara granosa shells, obtained from a local market, were cleaned and air-dried for a few days. About 20 g of cleaned shells were manually ground and milled for 3 h, with no heat treatment, designated as CS. Other samples were prepared by heating the shells in a Vulcan muffle furnace at 600 and 1000°C, and were designated as NC6 and NC10, respectively. The samples were cooled to room temperature, then manually ground and milled using a planetary mill (Pulverisette 6) for 3 h. The resulting material was stored in a sample bottle for further use and characterisation.

2.2. Characterisation. Powder X-ray diffraction (PXRD) patterns of the samples were recorded on a Shimadzu XRD-6000 powder diffractometer using CuK_α radiation (λ = 0.15406 Å) at 40 kV, 30 mA at 4°C min^{-1}. The BET surface area of the samples was determined by a Quantachrome AS1Win surface area and pore-size analyser using the nitrogen gas adsorption-desorption technique at 77 K together with the BET equation. A field-emission-scanning electron microscope (FEI Nova Nanosem 230) was used to study the surface morphology of the samples. To examine the cross-sectional image of the samples, a transmission electron microscope (Hitachi H7100 TEM) was used. Raman studies were performed using an HeNe 20 mW laser of wavelength 514 nm in a Perkin Elmer Raman Micro 200 spectrometer.

2.3. Experimental Design of the CNTs Synthesis. The experimental design was developed and optimised using response surface methodology (RSM). RSM utilises mathematical and statistical techniques to perform modelling and analysis of problems in which a response of interest is influenced by several variables. The objective is to optimise the response from the selected variables [20]. A standard RSM design, called a central composite design (CCD) was applied to develop the experimental design for the synthesis of CNTs using *Anadara granosa* shells as the substrate.

There are three operating conditions performed in this work, namely the catalyst percentage loading, duration of reaction, and reaction temperature as illustrated in Table 1. The variables ranges were selected based on the results obtained from the preliminary studies and the literature [21–23]. For three variables (n = 3), the total number of experiments were 20, which was determined by the expression 2^n (2^3 = 8 factorial points), 2n (2 × 3 = 6 axial points), six (centre points, six replications). The axial points are located at $(\pm\alpha, 0, 0)$, $(0, \pm\alpha, 0)$, and $(0, 0, \pm\alpha)$, where α is the distance of the axial points from centre. In this study, the value of α for the CCD was fixed at 1.73205 to get a rotatable design [20]. The complete design matrices of the experimental runs are given in Table 2. All the parameters at the zero level represent the centre points. The experimental runs were randomised to minimise the effects of uncontrolled factors such as human error. RSM analysed the experimental data obtained from the above procedure by following a second-order polynomial as follows [20]:

Table 1: Range and levels of the variables for CNTs synthesis.

Variables	Code	Unit	Levels	
			Low	High
Catalyst percentage	A	wt.%	5	10
Synthesis temperature	B	°C	700	1000
Synthesis duration	C	h	0.25	1.00

$$Y = b_0 + \sum_{i=1}^{n} b_i x_i + \sum_{i=1}^{n} b_{ii} x_i^2 + \sum_{i=1}^{n-1} \sum_{j=i+1}^{n} b_{ij} x_i x_j, \quad (1)$$

where Y is the predicted response (% carbon yield), b_0, b_i, b_{ii}, and b_{ij} are the constant, linear, quadratic, and interaction coefficients, respectively, whereas x_i and x_j are the uncoded independent variables. Regression analysis and analysis of variance (ANOVA) were performed using Design Expert software version 8.05 (STAT-EASE Inc., Minneapolis, USA). The fitted quadratic polynomial equation obtained from the regression analysis was used to develop the response surfaces and contour plots. The carbon yield of each catalytic reaction was measured by calculating the carbon yield percentage (%C) as specified [24] below

$$\%C = \frac{m_{\text{after}}^{\text{cat}} - m_{\text{before}}^{\text{cat}}}{m_{\text{before}}^{\text{cat}}} \cdot 100\%. \quad (2)$$

2.4. CNTs Synthesis. The process optimisation of CNTs synthesis using *Anadara granosa* shells as the catalyst support was studied by first dissolving a desired amount (w/w%) of metal salt, $Fe(NO_3)_3 \cdot 9H_2O$ (HmbG), into distilled water. The iron catalyst was impregnated on the calcite by direct addition of calcite into the metal salt solution. The resulting mixture was continuously stirred and heated to evaporate the solvent. The resulting material was dried at 60°C, overnight and kept in a sample bottle for further use and characterisations. The decomposition of hexane was carried out in a horizontal furnace at 850°C. Approximately 1 g of the prepared catalyst was placed in an alumina boat and inserted into a quartz tube under nitrogen flow at 100 mL/min and heated at 850°C for 1 h, followed by a flow of hexane at 0.06 mL/min for 1 h. The product was cooled under a nitrogen flow and stored in a sample bottle for further use and characterisation. The final product was purified using 30% HNO_3 by the sonication method.

3. Results and Discussion

3.1. Characterisation of the As-Prepared Catalyst. The XRD patterns of the cockle shells before- and after- heat treatment were studied in order to identify the phase transformation. The XRD patterns of the as-prepared powders of blood-cockle shells (Figure 1(a)) showed that it was of aragonite phase (JCPDS card no. 5-0453). The XRD pattern of the sample heated at 600°C (Figure 1(b)) showed that it was

Table 2: Experimental design matrix and results for process optimization.

Run	Catalyst percentage, A (%)	Synthesis temperature, B (°C)	Synthesis duration, C (h)	CNTs yield (%)
1	5.0	1000	0.5	75.33
2	10.0	1000	1.0	98.45
3	10.0	700	1.0	86.78
4	10.0	1000	0.5	88.34
5	10.0	700	0.5	72.34
6	5.0	700	1.0	70.89
7	5.0	1000	1.0	85.32
8	5.0	700	0.5	69.03
9	7.5	1110	0.8	90.23
10	7.5	850	0.3	90.23
11	3.2	850	0.8	60.46
12	7.5	850	1.2	133.51
13	11.8	850	0.8	80.34
14	7.5	590	0.8	46.42
15	7.5	850	0.8	125.77
16	7.5	850	0.8	121.45
17	7.5	850	0.8	133.93
18	7.5	850	0.8	127.98
19	7.5	850	0.8	131.62
20	7.5	850	0.8	128.44

a pure calcite phase (JCPDS card no. 83-0578) with the strongest reflections at $2\theta = 29.84°$, 47.91°, and 48.94°. On the other hand, the sample heated at 1000°C (Figure 1(c)) showed three strong reflections at $2\theta = 37.68°$, 54.18°, and 32.52°, which were identified as calcium oxide, CaO (JCPDS Card No. 37-1497). At this temperature, the calcite was completely decomposed into calcium oxide and no trace of the calcite phase could be detected. This shows that phase transformations from aragonite to calcite and calcium oxide took place when the cockle shells were heated to 600 and 1000°C, respectively.

Figure 2(a) shows the XRD patterns of the calcite impregnated with the iron catalyst. The CNTs phase of (002) reflection with the substrate already transformed to calcium oxide (CaO) after the decomposition of hexane is shown in Figure 2(b). In addition, the α-Fe phase was also detected. This shows that the iron nitrate was converted to the α-Fe phase as a result of thermal treatment [25]. After purification using HNO_3, the peaks corresponding to the CNTs phase were sharper; no CaO peaks can be clearly observed (Figure 2(c)). FESEM micrographs of the as-prepared catalyst used are shown in Figure 3(a), showing that the iron particles were well-dispersed and attached to the substrate as confirmed by EDX analysis (Figure 3(b)).

3.2. Optimisation of CNTs Synthesis. A central composite design (CCD) was used to develop a correlation between the factors affecting CNTs synthesis and the carbon-yield

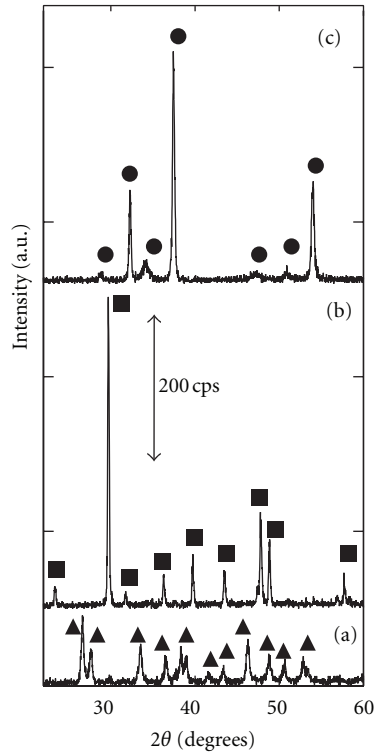

Figure 1: XRD patterns of cockle shells (*Anadara granosa*) before heat treatment (a) and after heat treatment at 600°C (b) and 1000°C (c), with the phases involved, aragonite (▲), calcite (■) and calcium oxide (•).

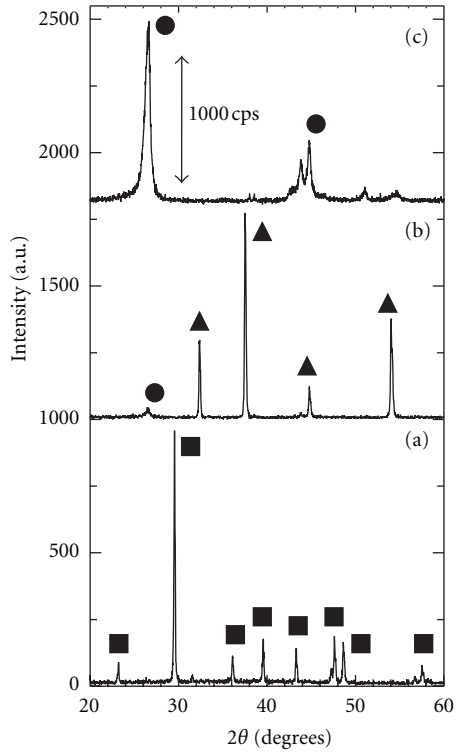

Figure 2: XRD patterns of calcite-supported iron catalyst (a), as-synthesised carbon nanotubes, CNT before purification (b) and CNTs after purification (c), calcite (■), α-Fe (♦) CaO (▲) and CNTs (•).

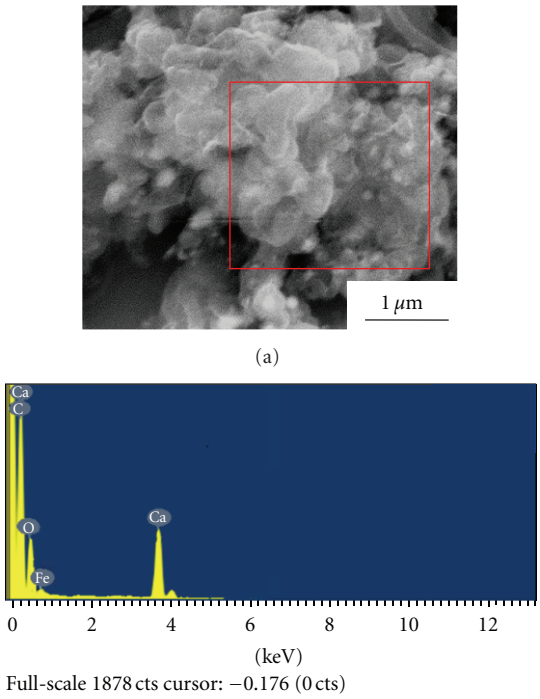

Figure 3: The FESEM micrograph of the as-prepared catalyst with well-dispersed iron particles (a), and the EDX analysis of the resulting catalyst (b).

percentage (%C). The complete design matrix and response for CNTs synthesis are presented in Table 2. The values of CNTs yield ranged from 46.42 to 134.51 wt%. Six replicates at the centre point of the design (Runs 15 to Run 20) were used to determine the experimental error [26].

3.3. Regression Analysis. Regression analysis is the general approach to fit the empirical model with the collected response variables for simulating and analysing variables, with a focus on the relationship between the dependent variable and one or more independent variables [20]. By using regression analysis, the responses obtained in Table 2 were correlated with the three independent factors using the polynomial equation given as (1). By taking their coded values, the model is expressed by:

$$\%C = +128.66 + 5.70A + 8.08B + 8.88C + 1.59AB + 0.87AC + 0.48BC - 19.90A^2 - 5.91B^2 - 20.60C^2. \quad (3)$$

Summaries of the analysis of variance (ANOVA) results are tabulated in Table 3. The Model F-value of 28.48 suggests that the model is significant; there is only a 0.01% chance that a model with an F-value this large could occur due to noise. Values of "Prob. > F" less than 0.0500 indicates that the model terms are significant. For CNTs synthesis, the model terms A, B, C, A^2, B^2, and C^2 significantly affected the measured response of the system (carbon yield). It was also observed that the linear terms of synthesis temperature (B) and synthesis duration (C) had a large effect on the CNTs yield due to the high F-value (Table 3). However, the interaction of the factors in this model did not contribute significant effect to the CNTs yield, as the values of "Prob. > F" for the interaction terms were greater than 0.1000.

Table 3: Analysis of variance (ANOVA) for response surface quadratic model.

Source	SS	df	Mean sq.	F-value	Prob. > F	Remarks
Model	13925.84	9	1547.32	27.10	<0.0001	significant
A	454.38	1	454.38	7.96	0.0200	significant
B	1091.27	1	1091.27	19.11	0.0018	significant
C	900.07	1	900.07	15.76	0.0033	significant
A^2	6049.78	1	6049.78	105.96	<0.0001	significant
B^2	6490.59	1	6490.59	113.68	<0.0001	significant
C^2	461.03	1	461.03	8.08	0.0194	significant
AB	6.020	1	6.020	0.11	0.7528	
AC	20.16	1	20.16	0.35	0.5670	
BC	1.80	1	1.80	0.03	0.8628	

SS: sum of squares; df: degree of freedom; Mean sq.: mean square.

The coefficient of determination, R^2, for CNTs synthesis using *Anadara granosa* shells was excellent at 0.9661. The high R^2 value indicates that the obtained model gives good system response estimates within the studied range. A relatively lower value of the coefficient of variation (CV of 7.69%) also indicates better precision and reliability of the experimental runs [27]. The CV is a measure of the reproducibility of the model. As a general rule, a model can be considered reasonably reproducible if its CV is not greater than 10% [28]. The adequate precision value of 14.106 for the model is substantially above 4.0, which also indicates adequate model discrimination [29].

Several diagnostic plots were studied to check the model's adequacy. Figure 4(a) shows the normal plot of residuals for CNTs synthesis. The residuals fall on a straight line, which indicates that errors are distributed normally for all responses. Figure 4(b) shows a random scatter plot of residuals versus predicted carbon yield, without any apparent patterns or unusual structure. This demonstrates that the proposed model is adequate. Figure 4(c) shows that the predicted values were close to the experimental values. It can be said that the developed model is able to effectively express the correlation between the reaction parameters and the carbon yield obtained from the decomposition of hexane.

3.4. Model Analysis. The results of the regression analysis demonstrate that carbon yield was significantly affected by the main factors, which were catalyst-loading percentage (A), duration of synthesis (B), synthesis temperature (C), and the higher-order terms of all the main factors. Figure 5(a) shows the three-dimensional response surface plot on the effects of the CNTs synthesis condition variables, which were catalyst percentage (A) and duration of synthesis (B), on carbon yield. It was observed that carbon yield increased with an increase in the duration of synthesis. Generally,

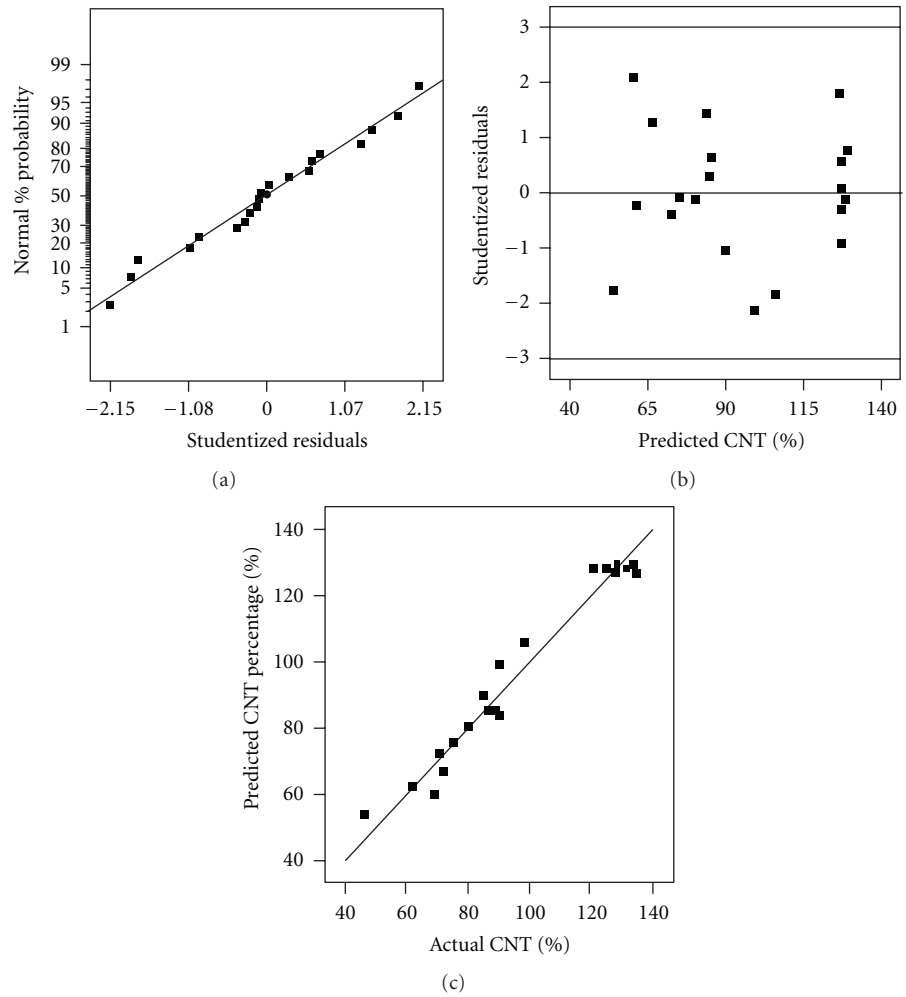

Figure 4: (a) Normal plot of residuals for carbon product. (b) Residuals versus predicted for carbon product. (c) Predicted versus actual plot for carbon product.

the duration of contact time between the catalyst and the hexane had a significant positive effect on CNTs synthesis. A higher conversion of hexane to solid carbon was favoured below 850°C and 7.5%, and decreased substantially as the deposition time increased. The metal-saturated support led to this observation. The limited sites of the catalyst produced no CNTs although the contact time with hexane was increased.

The effect of the duration of synthesis and catalyst percentage on CNTs synthesis was studied (Figure 5(b)). It can be seen that carbon yield increased with an increase in the catalyst percentage at lower temperatures. This observation suggests that the as-prepared catalyst became more active with a higher metal content as the temperature increased. This happened since the formation of CNTs was closely correlated with the available carbon source and the active sites of the catalytic metal particles. After subsequently reaching a stable level, the carbon yield started to decrease even though the catalyst percentage increased, because the contact time limited the available carbon source. Considering the efficiency of the catalytic metal, the catalyst at 7.5% loading yielded the optimum contact time of 45 min. Elevated temperature also played an important role in inhibiting CNTs growth. Although it has been previously reported that elevated temperature tend to produce a higher carbon yield since it has a great impact on the activity of metals and the decomposition of carbon-containing gases, overly high temperature may result in the agglomeration of catalytic metal particles and becomes a negative factor in CNTs formation [30]. Hence, a moderate temperature is essential for obtaining a high yield. According to this study, the optimum temperature to synthesize the CNTs is 850°C.

3.5. Process Optimisation of CNTs Synthesis. The numerical optimisation method is used to optimise the desired response of the system, which is the carbon yield, while maintaining all the variables in the range of the experimental values. The optimised conditions and predicted carbon yields are provided in Table 4. Using this optimised solution, the experimental run for CNTs synthesis was conducted accordingly for verification; the experimental value obtained was 131.62%. This result suggests that the experimental value is very close to the value calculated from the model, which consequently verifies the potential of the model.

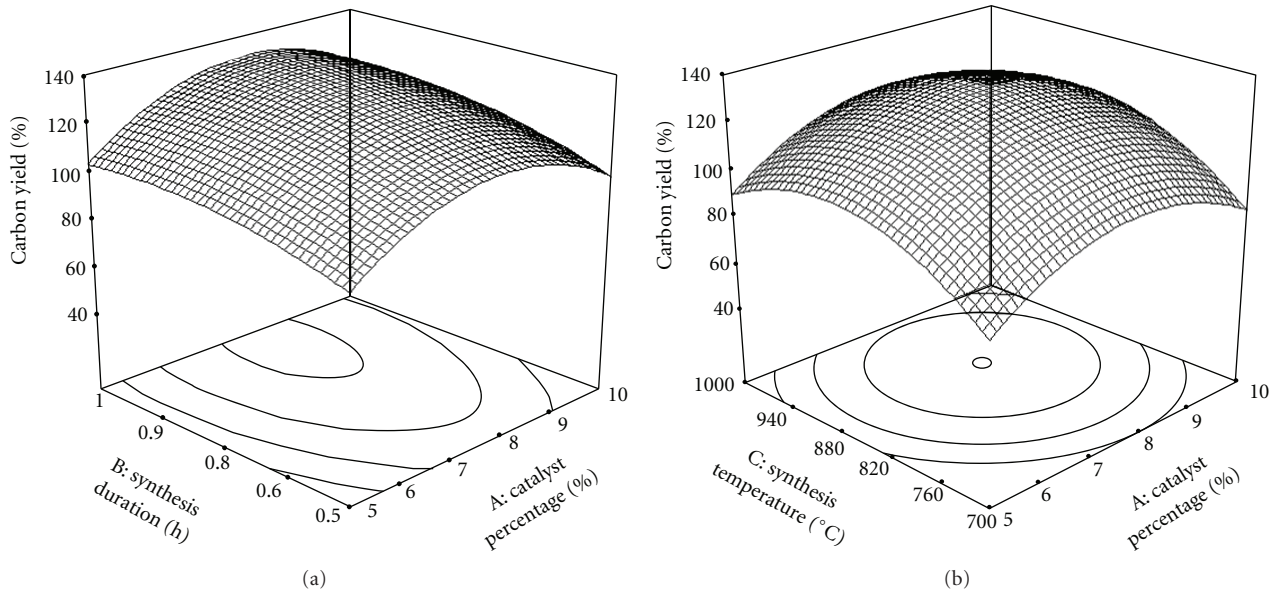

Figure 5: (a) Three-dimensional response surface plot of CNTs percentage (effect of varying catalyst percentage and synthesis duration, synthesis temperature = 850°C min). (b) Three-dimensional response surface plot of CNTs percentage (effect of varying catalyst percentage and synthesis temperature, synthesis duration = 45 min).

Table 4: Optimization criteria for CNTs synthesis using *Anadara granosa* shells as substrate.

Reaction conditions	
Catalyst percentage (%)	7.5
Synthesis duration (h)	0.75
Synthesis temperature (°C)	850
Predicted carbon yield (%)	129.22
Experimental carbon yield (%)	131.62

3.6. Purification and Characterisation. The typical FESEM and TEM images of both the as-prepared and purified CNTs are shown in Figure 6. Figure 6(a) shows FESEM micrographs of the as-prepared CNTs, showing the presence of a large proportion of CNTs bundles between the CaO lumps. CaO lumps were obtained as the calcite phase was transformed to CaO upon heating to a temperature higher than 700°C, as discussed earlier. Figure 6(b) shows no CaO lumps present with the purified CNTs after acid treatment of the sample. The CNTs were highly agglomerated in the purified sample, since no support was present to keep them apart. Figure 6(c) shows the TEM images of CNTs from the raw untreated sample, showing that the products contained large calcite particles, as shown by the black fringes. The image also shows the typical tubular wall structure of CNTs. From the TEM images, we observed that the CNTs were mostly around 30–100 nm in diameter. In addition, carbon nanofibres (CNFs) could be also observed, as shown in Figure 6(d).

The nitrogen adsorption isotherms of the CNTs samples (after purification using an acid treatment) were carried out while keeping the samples isothermal at 77 K. Figure 7(a) shows that the nitrogen adsorption isotherm of the CNTs is a mixture of Type I (inset of Figure 7(a)) and Type II according to the IUPAC classification [31]. The BJH pore-size distribution (Figure 7(b)) indicates the presence of micropores, in agreement with the Type I isotherm, with pore sizes centred at around 24 nm. The BET-specific surface area and pore volumes of the sample were calculated to be about 525 m^2/g and 0.53 cm^3/g, respectively.

The graphitic nature of the CNTs was probed using Raman spectra as shown in Figure 8. The G band which was detected at 1578 cm^{-1} corresponds to movement in the opposite direction of two neighbouring carbon atoms in a graphene sheet [32]. The band at 1351 cm^{-1} was assigned to the D mode, attributed to defects in the tube ends, staging disorders, and curved graphene layers [30]. The intensity ratio of I_D/I_G is known to be dependent on the structural characteristics of CNTs, and is frequently used to determine the quality of CNTs [30]. The I_D/I_G values of the CNTs before and after the purification step were 0.86 and 0.88, respectively, which suggested a defective structure or a lower graphitisation degree in the resulting CNTs. It was also found that the purification step using acid had very little impact on CNTs structure.

4. Conclusions

The process optimisation for CNT synthesis using *Anadara granosa* shells as the catalyst support has provided promising results with 131.62% carbon yield. Generally, the analysis suggests that CNT formation via the decomposition of hexane was significantly influenced by three main factors, namely catalyst percentage, synthesis temperature, and the duration of reaction. Under our experimental setup, the optimum conditions were obtained at a total iron loading of 7.5%, with a 45 min reaction time and at a temperature

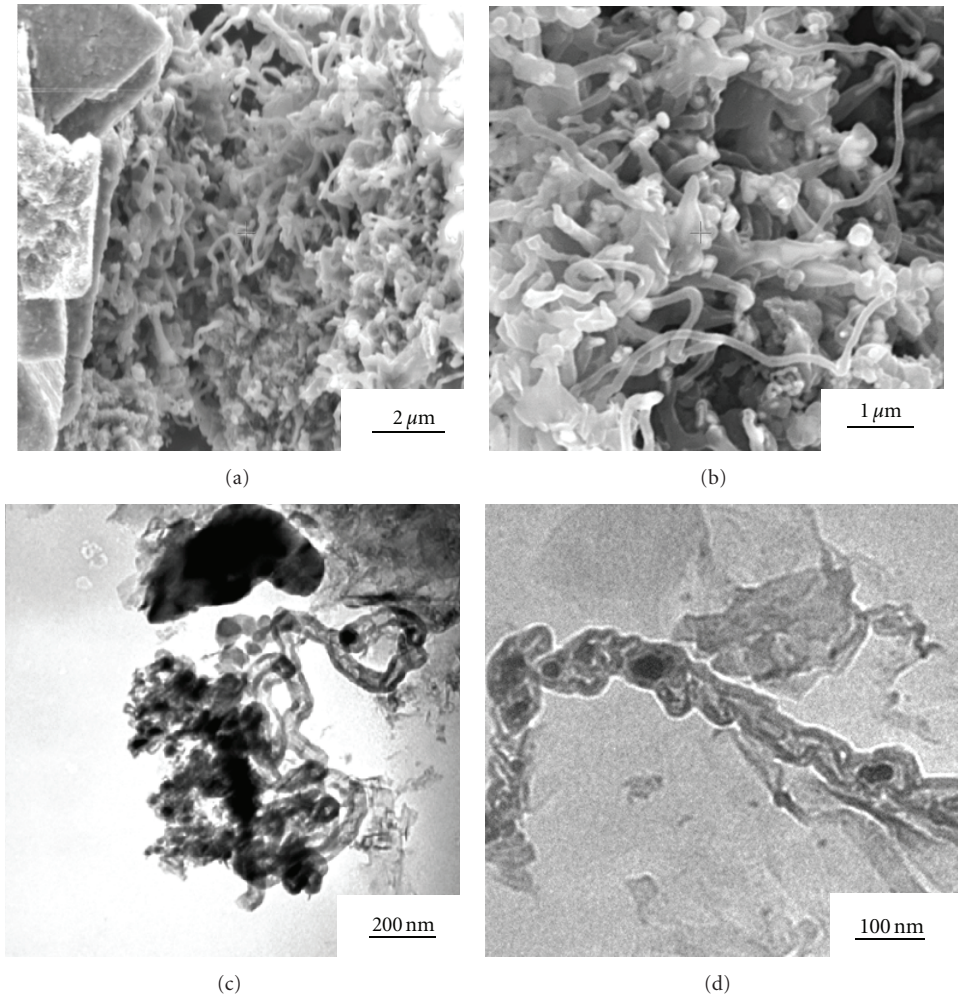

Figure 6: The FESEM micrograph of the carbon nanotubes (CNTs) before HNO_3 purified (a) and the FESEM (b) and TEM (c) micrographs of the CNTs after HNO_3 purified. Carbon nanofibres (CNFs) could be also observed from the TEM observations (d).

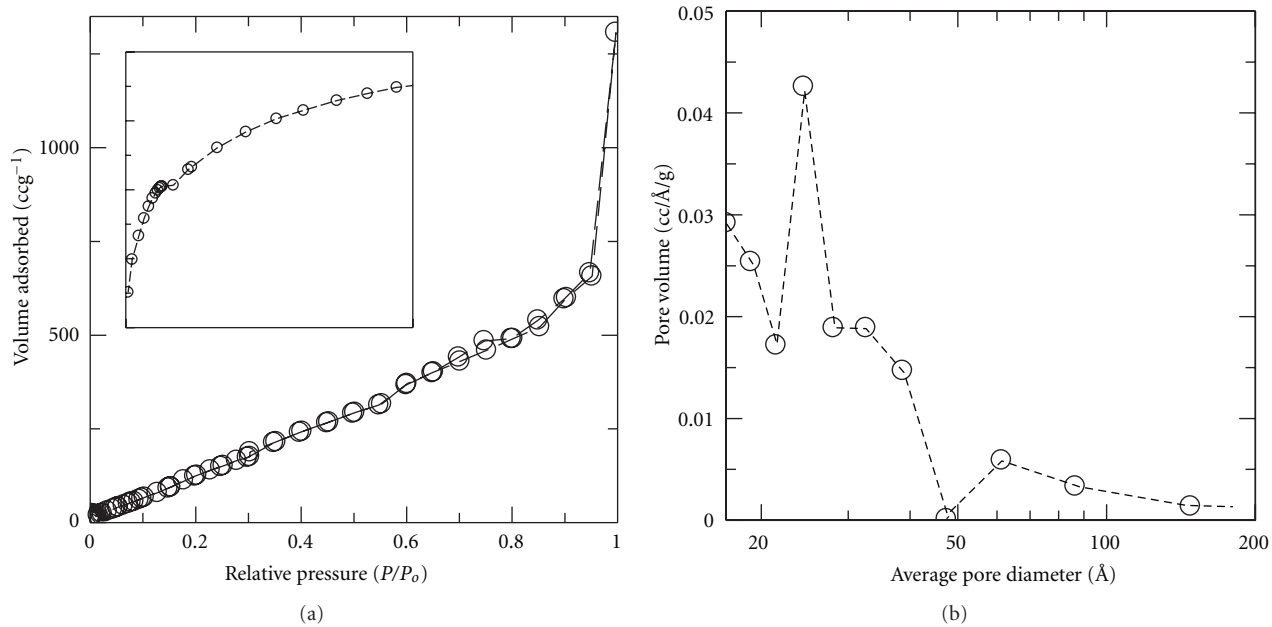

Figure 7: Nitrogen adsorption-desorption isotherms with the micropore region inset (a) and their corresponding BJH pore-size distribution (b) of the CNTs synthesized at optimum conditions.

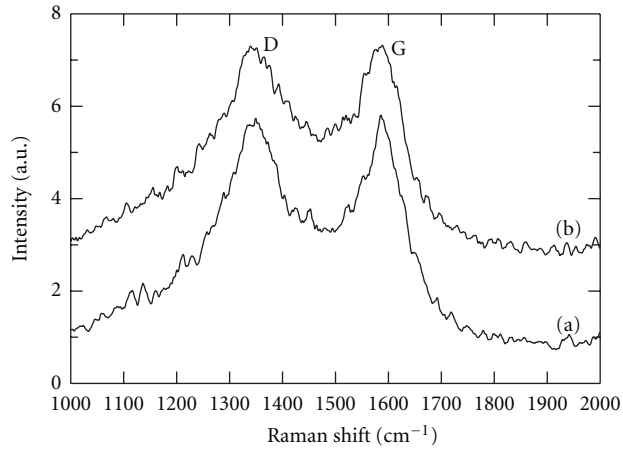

Figure 8: Raman spectra of CNTs synthesized at optimum conditions, before (a) and after (b) HNO_3 purified.

of 850°C. The catalyst and catalyst precursors can be easily prepared from *Anadara granosa* shells which are a promising substrate for large-scale and low-cost production of CNTs with simple one-step purification.

Acknowledgments

The authors wish to acknowledge the research facilities and financial support provided through the Research University Grant Scheme (RUGS) [05-01-09-0809RU Vote: 91814] and the Special Graduate Research Allowance (SGRA) for S. A. Zakarya under the same vote number from Universiti Putra Malaysia, UPM.

References

[1] S. Iijima, "Helical microtubules of graphitic carbon," *Nature*, vol. 354, no. 6348, pp. 56–58, 1991.

[2] A. Odani, A. Nimberger, B. Markovsky et al., "Development and testing of nanomaterials for rechargeable lithium batteries," *Journal of Power Sources*, vol. 119–121, pp. 517–521, 2003.

[3] A. C. Dillon, K. M. Jones, T. A. Bekkedahl, C. H. Kiang, D. S. Bethune, and M. J. Heben, "Storage of hydrogen in single-walled carbon nanotubes," *Nature*, vol. 386, no. 6623, pp. 377–379, 1997.

[4] Y. Nakayama and S. Akita, "Field-emission device with carbon nanotubes for a flat panel display," *Synthetic Metals*, vol. 117, no. 1–3, pp. 207–210, 2001.

[5] C. Cantalini, L. Valentini, I. Armentano, J. M. Kenny, L. Lozzi, and S. Santucci, "Carbon nanotubes as new materials for gas sensing applications," *Journal of the European Ceramic Society*, vol. 24, no. 6, pp. 1405–1408, 2004.

[6] J. H. Chen, W. Z. Li, D. Z. Wang, S. X. Yang, J. G. Wen, and Z. F. Ren, "Electrochemical characterization of carbon nanotubes as electrode in electrochemical double-layer capacitors," *Carbon*, vol. 40, no. 8, pp. 1193–1197, 2002.

[7] J. Qiu, Y. Li, Y. Wang et al., "High-purity single-wall carbon nanotubes synthesized from coal by arc discharge," *Carbon*, vol. 41, no. 11, pp. 2170–2173, 2003.

[8] Z. Jia, Z. Wang, J. Liang, B. Wei, and D. Wu, "Production of short multi-walled carbon nanotubes," *Carbon*, vol. 37, no. 6, pp. 903–906, 1999.

[9] J. H. Lin, C. S. Chen, M. H. Rümmeli et al., "Growth of carbon nanotubes catalyzed by defect-rich graphite surfaces," *Chemistry of Materials*, vol. 23, no. 7, pp. 1637–1639, 2011.

[10] W. Wang, S. Kunwar, J. Y. Huang, D. Z. Wang, and Z. F. Ren, "Low temperature solvothermal synthesis of multiwall carbon nanotubes," *Nanotechnology*, vol. 16, no. 1, pp. 21–23, 2005.

[11] S. Manafi, M. B. Rahaei, Y. Elli, and S. Joughehdoust, "High-yield synthesis of multi-walled carbon nanotube by hydrothermal method," *Canadian Journal of Chemical Engineering*, vol. 88, no. 2, pp. 283–286, 2010.

[12] M. H. Rümmeli, F. Schäffel, C. Kramberger et al., "Oxide-driven carbon nanotube growth in supported catalyst CVD," *Journal of the American Chemical Society*, vol. 129, no. 51, pp. 15772–15773, 2007.

[13] E. Couteau, K. Hernadi, J. W. Seo et al., "CVD synthesis of high-purity multiwalled carbon nanotubes using $CaCO_3$ catalyst support for large-scale production," *Chemical Physics Letters*, vol. 378, no. 1-2, pp. 9–17, 2003.

[14] C. J. Lee and J. Park, "Growth model for bamboolike structured carbon nanotubes synthesized using thermal chemical vapor deposition," *Journal of Physical Chemistry B*, vol. 105, no. 12, pp. 2365–2368, 2001.

[15] Ç. Öncel and Y. Yürüm, "Carbon nanotube synthesis via the catalytic CVD method: a review on the effect of reaction parameters," *Fullerenes Nanotubes and Carbon Nanostructures*, vol. 14, no. 1, pp. 17–37, 2006.

[16] S. S. Dang and X. W. Chen, "Natural lavas as catalysts for efficient production of carbon nanotubes and nanofibers," *Angewandte Chemie—International Edition*, vol. 46, no. 11, pp. 1823–1824, 2007.

[17] J. P. Cheng, X. B. Zhang, Y. Ye et al., "Production of carbon nanotubes with marine manganese nodule as a versatile catalyst," *Microporous and Mesoporous Materials*, vol. 81, no. 1–3, pp. 73–78, 2005.

[18] O. M. Dunens, K. J. Mackenzie, and A. T. Harris, "Synthesis of multiwalled carbon nanotubes on fly ash derived catalysts," *Environmental Science and Technology*, vol. 43, no. 20, pp. 7889–7894, 2009.

[19] A. Magrez, J. W. Seo, C. Mikó, K. Hernádi, and L. Forró, "Growth of carbon nanotubes with alkaline earth carbonate as support," *Journal of Physical Chemistry B*, vol. 109, no. 20, pp. 10087–10091, 2005.

[20] D. C. Montgomery, E. A. Peck, G. G. Vining, and J. Vining, *Introduction to Linear Regression Analysis*, John Wiley & Sons, New York, NY, USA, 2001.

[21] G. S. B. McKee, C. P. Deck, and K. S. Vecchio, "Dimensional control of multi-walled carbon nanotubes in floating-catalyst CVD synthesis," *Carbon*, vol. 47, no. 8, pp. 2085–2094, 2009.

[22] J. B. Bult, W. G. Sawyer, P. M. Ajayan, and L. S. Schadler, "Passivation oxide controlled selective carbon nanotube growth on metal substrates," *Nanotechnology*, vol. 20, no. 8, Article ID 085302, 2009.

[23] C. E. Baddour, F. Fadlallah, D. Nasuhoglu, R. Mitra, L. Vandsburger, and J. L. Meunier, "A simple thermal CVD method for carbon nanotube synthesis on stainless steel 304 without the addition of an external catalyst," *Carbon*, vol. 47, no. 1, pp. 313–318, 2009.

[24] L. Vanyorek, D. Loche, H. Katona et al., "Optimization of the catalytic chemical vapor deposition synthesis of multiwall carbon nanotubes on $FeCo(Ni)/SiO_2$ aerogel catalysts by statistical design of experiments," *Journal of Physical Chemistry C*, vol. 115, no. 13, pp. 5894–5902, 2011.

[25] J. W. An and D. S. Lim, "Synthesis and characterization of alumina/carbon nanotube composite powders," *Journal of Ceramic Processing Research*, vol. 3, no. 3, pp. 174–177, 2002.

[26] X. Yuan, J. Liu, G. Zeng, J. Shi, J. Tong, and G. Huang, "Optimization of conversion of waste rapeseed oil with high FFA to biodiesel using response surface methodology," *Renewable Energy*, vol. 33, no. 7, pp. 1678–1684, 2008.

[27] J. A. Cornell and A. I. Khuri, *Response Surfaces: Designs and Analyses*, Marcel Dekker, New York, NY, USA, 1987.

[28] Q. K. Beg, V. Sahai, and R. Gupta, "Statistical media optimization and alkaline protease production from *Bacillus mojavensis* in a bioreactor," *Process Biochemistry*, vol. 39, no. 2, pp. 203–209, 2003.

[29] M. Y. Noordin, V. C. Venkatesh, S. Sharif, S. Elting, and A. Abdullah, "Application of response surface methodology in describing the performance of coated carbide tools when turning AISI 1045 steel," *Journal of Materials Processing Technology*, vol. 145, no. 1, pp. 46–58, 2004.

[30] J. Cheng, X. Zhang, Z. Luo et al., "Carbon nanotube synthesis and parametric study using CaCO3 nanocrystals as catalyst support by CVD," *Materials Chemistry and Physics*, vol. 95, no. 1, pp. 5–11, 2006.

[31] K. S. W. Sing, D. H. Everett, R. A. W. Haul et al., "Reporting physisorption data for gas/solid systems," in *Handbook of Heterogeneous Catalysis*, 1985.

[32] H. Hiura, T. W. Ebbesen, K. Tanigaki, and H. Takahashi, "Raman studies of carbon nanotubes," *Chemical Physics Letters*, vol. 202, no. 6, pp. 509–512, 1993.